Determination of the ^{239}Np (n, f) and ^{240}Np(n, f) cross sections using the surrogate reaction method

V. V. Desai,* B. K. Nayak, A. Saxena, E. T. Mirgule, and S. V. Suryanarayana
Nuclear Physics Division, Bhabha Atomic Research Centre, Mumbai 400 085, India
(Received 3 June 2013; published 29 July 2013)

The surrogate reaction method has been used to determine neutron-induced fission cross sections of the short-lived minor actinides ^{239}Np and ^{240}Np in the equivalent neutron energy range of 10.5–16.5 and 9.0–16.0 MeV, respectively. The ^{240}Np and ^{242}Pu compound nuclei are produced at similar excitation energies in ^{238}U(^{6}Li, αf)^{240}Np and ^{238}U(^{6}Li, df)^{242}Pu transfer reactions at $E_{lab} = 39.6$ MeV. The fission decay probabilities of ^{240}Np [surrogate of ^{239}Np(n, f)] and ^{242}Pu [surrogate of ^{241}Pu(n, f)] compound systems have been measured experimentally as a function of excitation energy to determine ^{239}Np(n, f) cross sections within the framework of hybrid surrogate ratio method by considering directly measured ^{241}Pu(n, f) cross sections as reference. Similarly, ^{238}U(^{7}Li, αf)^{241}Np and ^{238}U(^{7}Li, tf)^{242}Pu transfer reactions at $E_{lab} = 41.0$ MeV have been used to determine ^{240}Np(n, f) cross sections. The present results for ^{239}Np(n, f) cross sections have been compared with recently reported ^{239}Np(n, f) cross sections obtained by the surrogate ratio method using ^{236}U(^{3}He, p) and ^{238}U(^{3}He, p) reactions [2] and also have been compared with the predictions of the statistical model code EMPIRE-3.1 for the fission barriers obtained from the barrier formula and the evaluated nuclear data libraries such as JENDL-4.0 and ENDF/B-VII.1. The present experimental results for ^{239}Np(n, f) and ^{240}Np(n, f) cross sections are found to be reasonably consistent with the EMPIRE-3.1 predictions.

DOI: 10.1103/PhysRevC.88.014613 PACS number(s): 24.50.+g, 24.87.+y, 25.85.Ec, 28.20.−v

I. INTRODUCTION

Neutron cross sections have been measured over the past 70 years and techniques are being continually developed to improve the accuracy and to extend the neutron cross-section data for both stable and radioactive nuclei. Neutron-induced fission cross sections of short-lived minor actinide nuclei are crucial for fundamental nuclear physics and also for applications in areas such as reactor physics and astrophysics [1]. In particular, these data are important for nuclear-waste transmutation using fast neutrons. However, very often the high radioactivity of the samples makes the direct measurement of these cross sections extremely difficult.

The ^{239}Np(n, f) and ^{240}Np(n, f) cross sections play an important role in the proliferation-resistance aspect of a reactor design, as ^{239}Np and ^{240}Np are produced on the way to ^{239}Pu and ^{240}Pu and further higher mass actinides. Precise information about the (n, f) cross sections for ^{239}Np and ^{240}Np in relation to their neutron capture cross section would help to predict the amount of ^{239}Pu and ^{240}Pu produced in a reactor [2]. Also these cross sections are highly relevant for the design of fast reactors/Accelerator Driven System capable of incinerating minor actinides. The challenge of directly obtaining the neutron-induced fission cross sections of ^{239}Np and ^{240}Np lies in their very short half-lives ($T_{1/2} = 2.356$ d and $T_{1/2} = 62$ min, respectively). The natural decay makes the sample very difficult to handle and produces a large background component in the measurements.

Often indirect methods such as the surrogate reaction method [3,4] involving a stable target and projectile are employed to estimate the compound nuclear cross sections for short-lived target nuclei. In Bohr's hypothesis, formation and decay of a compound nucleus are considered to be independent of each other; this independence is exploited in the surrogate-reaction approach. The compound nucleus (B*) occurring in the reaction of interest (a + A → B* → c + C) that involves difficult-to-produce targets is produced via an alternative reaction, called a surrogate reaction (d + D → B* + b), which involves a stable projectile-target combination (d + D) that is experimentally more feasible. The decay of B* is observed in coincidence with the outgoing direct-reaction particle b. The measured compound-nuclear decay probabilities can then be combined with calculated formation cross sections for the compound nucleus in the desired reaction to yield the relevant reaction cross section. In the actinide region, short-lived isotopes often have longer-lived neighbors that can be used as targets in the surrogate experiment. A charged particle reaction on these neighboring isotopes can be used to form the same compound nucleus as that of the desired neutron-induced reactions [5]. In the past, surrogate reaction methods in various forms such as the absolute surrogate method [3,4], the surrogate ratio method (SRM) [6–8], and the hybrid surrogate ratio method (HSRM) [9] have been employed to get indirect estimates of the neutron-induced reaction cross sections of many short-lived target nuclei. In the absolute surrogate method, the measured fission decay probabilities are simply multiplied by estimated neutron capture cross sections to deduce the (n, f) cross section. However, the limitation of this technique is due to the experimental determination of fission decay probability by the ratio of particle-fission coincident to particle single events $P_f(E_{ex}) = \frac{N_{x-f}}{N_x}$. The determination of $P_f(E_{ex})$ relies largely on the accurate determination of the particle singles counts N_x, which turns out to be the source of the largest uncertainty in the absolute surrogate measurement, due to practical problems of target contamination. The shortcomings of the absolute surrogate method have been eliminated in the SRM. In this method the ratio of the fission probabilities of two

*vvdesai@barc.gov.in

compound-nucleus reactions for the same excitation energy are determined experimentally. Knowing the cross section for one of the compound-nuclear reactions (reference reaction) then allows one to extract the other (desired reaction) by using the ratio $R(E_{ex})$ as follows:

$$\frac{\sigma_f^{n+A}(E_{ex})_{(desired)}}{\sigma_f^{n+B}(E_{ex})_{(reference)}} = R(E_{ex}) = \frac{\sigma_{CN}^{n+A}(E_{ex})}{\sigma_{CN}^{n+B}(E_{ex})} \frac{P_f^A(E_{ex})}{P_f^B(E_{ex})}, \quad (1)$$

where $\frac{P_f^A(E_{ex})}{P_f^B(E_{ex})}$ is the ratio of the decay probability of the two compound systems at the same excitation energy, which can be experimentally measured, and ratio of the neutron capture cross section for the corresponding target nuclei in the neutron-induced reaction at the same excitation energies, $\frac{\sigma_{n+A}^{CN}(E_{ex})}{\sigma_{n+B}^{CN}(E_{ex})}$, is calculated by using an optical model, thereby enabling one to find out the neutron-induced fission cross section for an unknown system.

More recently, the HSRM, which combines the absolute surrogate and surrogate ratio methods, has been developed and employed by Nayak *et al.* [9] to determine the ^{233}Pa$(n,\ f)$ cross sections in the equivalent neutron energy range of 11.5–16.5 MeV. In the SRM the two compound nuclei corresponding to "desired" and "reference" reactions are populated by performing the same surrogate reaction on two different targets, whereas in the HSRM one performs two surrogate reactions on the same target *in situ* in two different transfer reactions, where two compound nuclei corresponding to the "desired reaction" and the "reference reaction" are populated. The relative fission decay probabilities of the compound nuclei are measured experimentally to determine the cross sections of the desired compound nuclear reaction by using Eq. (1). In the HSRM, thus by taking a ratio of two reactions on the same target, systematic uncertainties due to target thickness, beam current, and dead time in the determination of the ratio of fission decay probabilities corresponding to "desired" and "reference" reactions are eliminated [9,10].

The validity of neutron-induced fission cross sections obtained by using the SRM has been questioned because of angular momentum and parity mismatch between the surrogate and desired reactions. In the SRM one assumes the decay probabilities of the compound nucleus to be independent of angular momentum and parity values, which is better known as the Weisskopf-Ewing approximation [11]. In the past, both experimental and theoretical studies have been carried out to investigate the validity of the Weisskopf-Ewing approximation in neutron-induced fission cross-section determination by the SRM. The determination of ^{236}U$(n,\ f)$ cross sections by the SRM has been shown to be consistent with ENDF/B-VII evaluations in the equivalent neutron energy range of 3.5–20 MeV [10], whereas below 3.5 MeV a strong angular momentum and parity influence has been observed. In the work of Lesher *et al.* [12], a similar conclusion has been drawn, where the ^{233}U$(n,\ f)$ cross sections are observed to be consistent with ENDF/B-VII evaluations for the equivalent neutron energy above 1 MeV but a large deviation from ENDF/B-VII data has been observed for neutron energies below 1 MeV. Moreover, studies carried out by Petit *et al.* [13] and Kessedjian *et al.* [14] are seen to be in excellent agreement with direct measurements even at very low energies ($E_n \leqslant$ 1 MeV). The validity of the Weisskoff-Ewing approximation has been investigated theoretically in the case of ^{235}U$(n,\ f)$ cross-section determination in the framework of the SRM by studying the angular momentum dependence of the fission decay probability ratio of ^{236}U and ^{234}U compound systems. Relatively good agreement is found between the simulated ratio results and the expected cross sections for energies above about 3 MeV. Discrepancies, as large as 50% occur at low energies ($E_n \leqslant$ 3 MeV), and they are about 25% near the threshold for second-chance fission [15]. In a more recent work, it has been shown that an accuracy of 3%–5% can be achieved in neutron-induced fission cross-section determination by using the SRM for nuclei in the uranium region at around 2.5–5.0 MeV with a difference of spin values between neutron-induced and surrogate reactions up to $10\hbar$ [16].

In the present work the $(n,\ f)$ cross sections for ^{239}Np and ^{240}Np have been determined using the HSRM, in the equivalent neutron energy range of 10.5–16.5 and 9–16 MeV, respectively. The ^{240}Np and ^{242}Pu compound nuclei are produced *in situ* at similar excitation energies in ^{238}U(^{6}Li, αf)^{240}Np and ^{238}U(^{6}Li, df)^{242}Pu transfer reactions at $E_{lab} = 39.6$ MeV for ^{239}Np$(n,\ f)$ cross-section determination. Similarly, the ^{238}U(^{7}Li, αf)^{241}Np and ^{238}U(^{7}Li, tf)^{242}Pu transfer reactions at $E_{lab} = 41.0$ MeV have been used to determine ^{240}Np$(n,\ f)$ cross sections. The ^{241}Pu$(n,\ f)$ cross sections have been used as standard reference in both cases. For ^{239}Np$(n,\ f)$ cross sections, there has been a recent measurement by Czeszumska *et al.* [2], employing the SRM in the equivalent neutron energy range of 1–20 MeV using ^{236}U(^{3}He, p) and ^{238}U(^{3}He, p) reactions, but the experimental data are not consistent with any of the evaluations such as ENDF/B-VII.0 [17], JENDL-4.0 [18], or CENDL-3.1 [19]. Moreover, there has been neither experimental measurement nor evaluated data available in the literature for the ^{240}Np$(n,\ f)$ cross sections.

II. EXPERIMENTAL DETAILS AND DATA ANALYSIS

Measurements were carried out using ^{6,7}Li beams obtained from the Bhabha Atomic Research Centre–Tata Institute of Fundamental Research (BARC-TIFR) Pelletron Accelerator Facility in Mumbai. The transfer reactions, their ground state Q values (Q_{gg}), and corresponding surrogate neutron-induced reactions are listed in Table I for the the present experiment. The two silicon surface barrier ΔE-E detector telescopes

TABLE I. Transfer reactions investigated in the present experiment, their ground state Q values (Q_{gg}), and corresponding surrogate neutron-induced reactions.

Transfer reaction	Q_{gg} (MeV)	Neutron-induced reaction
^{238}U(^{6}Li, α)^{240}Np*	6.656	^{239}Np$(n,\ f)$
^{238}U(^{6}Li, d)^{242}Pu*	−6.458	^{241}Pu(n,f)
^{238}U(^{7}Li, α)^{241}Np*	5.530	^{240}Np$(n,\ f)$
^{238}U(^{7}Li, t)^{242}Pu*	−7.45	^{241}Pu$(n,\ f)$

T_1 and T_2 with ΔE detectors of thicknesses of 150 and 100 μm, respectively, and with identical E detectors of thicknesses of 1.0 mm were mounted in a reaction plane at angles of 85° and 105° with respect to the beam direction to identify projectile-like fragments (PLFs). Aluminum foil of thickness of 3.86 mg/cm^2 was placed in front of the particle telescopes to stop the fission fragments and thereby protect the ΔE detectors from radiation damage. The PLFs (protons, deuterons, tritons and α particles) are uniquely identified by plotting the partial energy loss in the ΔE detector against the residual energy (E_{res}) in the E detector as reported earlier [8]. A large-area (450 mm^2) solid state detector was kept at an angle of 160° with respect to the beam direction and subtended a solid angle of 63 msr with an angular opening of 16° to detect fission fragments in coincidence with PLFs. The telescopes were energy calibrated by using a ^{228,229}Th source and in an in-beam experiment that made use of the discrete α-particle peaks corresponding to ^{15}N* states from the ^{12}C(^{7}Li, α)^{15}N* reaction at a ^{7}Li beam energy of 18.0 MeV [20,21].

In the first experiment, a self supporting ^{238}U target of thickness of 2.3 mg/cm^2 was bombarded with a ^{6}Li beam of energy $E_{lab} = 39.6$ MeV. The ^{240}Np and ^{242}Pu compound nuclei, formed in the ^{238}U(^{6}Li, α)^{240}Np (surrogate of $n+^{239}$Np $\rightarrow$ ^{240}Np) and ^{238}U(^{6}Li, d)^{242}Pu (surrogate of $n + ^{241}$Pu $\rightarrow$ ^{242}Pu) transfer reactions were identified by outgoing α and deuteron PLFs, respectively. The excitation energies (E_{ex}) of the compound nuclei ^{240}Np and ^{242}Pu have been determined on an event-by-event basis by employing two-body kinematics from α and deuteron energy spectra. The ground-state Q values, Q_{gg}, for ^{238}U(^{6}Li, α)^{240}Np and ^{238}U(^{6}Li, d)^{242}Pu are 6.656 and -6.458 MeV, respectively. Hence the ^{240}Np and ^{242}Pu compound systems are populated at overlapping excitation energies. The excitation energy spectra obtained for ^{240}Np and ^{242}Pu compound nuclei, with and without coincidence with fission fragments, are shown in Fig. 1. The ratio of PLF-fission coincidences to PLF single counts in ^{238}U(^{6}Li, α)^{240}Np and ^{238}Th(^{6}Li, d)^{242}Pu transfer reactions correspond to the fission decay probabilities $P_f^{^{240}Np}$ and $P_f^{^{242}Pu}$ of the compound systems ^{240}Np and ^{242}Pu respectively; as follows:

$$P_f^{CN} = \frac{N_{x_i - f}}{N_{x_i}}, \tag{2}$$

where x_i denotes the α or deuteron PLF channel corresponding to the ^{240}Np and ^{242}Pu compound systems. The ratios of coincidence to singles for α and deuteron counts are taken in steps of 0.5 MeV in the excitation energy range of 16.5–22.5 MeV and hence the ratio of fission decay probabilities, $\frac{P_f^{^{240}Np}(E_{ex})}{P_f^{^{242}Pu}(E_{ex})}$, of the compound systems ^{240}Np and ^{242}Pu is determined. Similarly, in the second experiment a ^{238}U target was bombarded with a ^{7}Li beam of energy $E_{lab} = 41$ MeV. The ^{241}Np and ^{242}Pu compound nuclei are formed in the ^{238}U(^{7}Li, α)^{241}Np (surrogate of $n+^{240}$Np $\rightarrow$ ^{241}Np) and ^{238}U(^{7}Li, t)^{242}Pu (surrogate of $n+^{241}$Pu $\rightarrow$ ^{242}Pu) reactions, respectively. The ground-state Q values, Q_{gg}, for ^{238}U(^{7}Li, α)^{241}Np and ^{238}U(^{7}Li, t)^{242}Pu are 5.530 and -7.45 MeV, respectively. Hence the ^{241}Np and ^{242}Pu compound systems are populated at overlapping excitation energies. The ratios of PLF-fission coincidence to

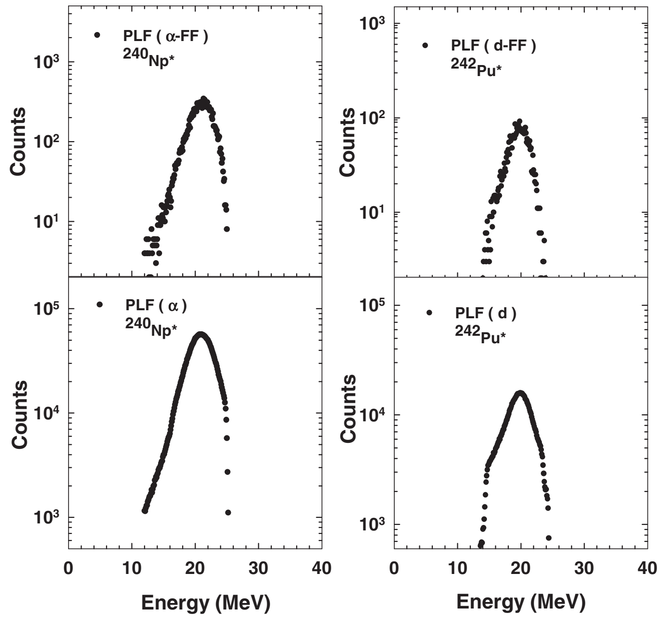

FIG. 1. Excitation energy spectra of compound systems ^{240}Np and ^{242}Pu produced in ^{238}U(^{6}Li, α)^{240}Np and ^{238}U(^{6}Li, d)^{242}Pu reactions, with and without coincidence with fission fragments, shown in the upper and lower panels, respectively.

PLF single counts for α particles and tritons have been taken in steps of 1.0 MeV in the excitation energy range of 15–22 MeV, and hence the ratios of fission decay probabilities of the compound systems ^{241}Np and ^{242}Pu, $\frac{P_f^{^{241}Np}(E_{ex})}{P_f^{^{242}Pu}(E_{ex})}$, are determined for each excitation energy bin. The ratios of fission decay probabilities, $\frac{P_f^{^{240}Np}(E_{ex})}{P_f^{^{242}Pu}(E_{ex})}$ and $\frac{P_f^{^{241}Np}(E_{ex})}{P_f^{^{242}Pu}(E_{ex})}$, are then multiplied by the ratio of the corresponding neutron-induced compound

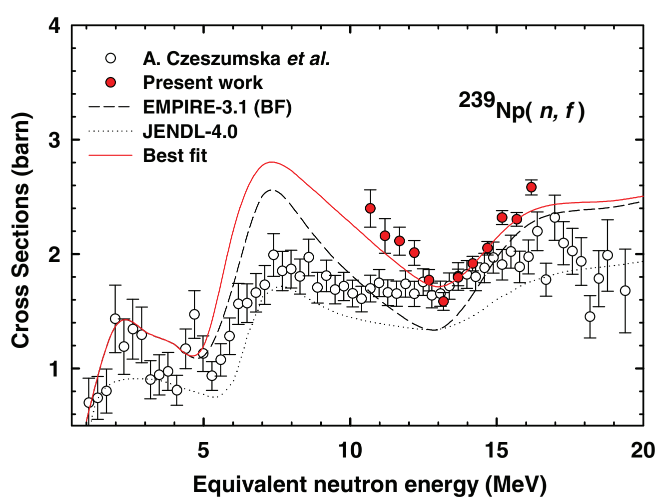

FIG. 2. (Color online) Experimental ^{239}Np(n, f) cross sections, present measurements (solid circles), and the work of Czeszumska *et al.* [2] (open circles). Calculated results are from the EMPIRE-3.1 code for fission barriers obtained from the barrier formula (BF) (short-dashed line). The adopted data from the JENDL-4.0 nuclear data library (dotted line) and the best fit (solid line) are also shown.

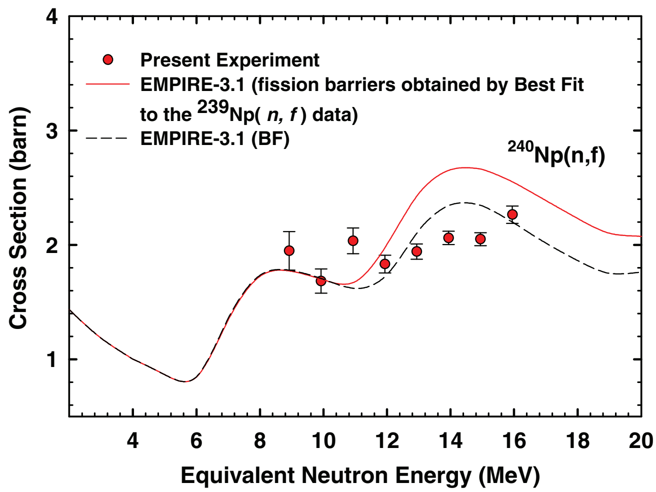

FIG. 3. (Color online) Experimental ^{240}Np(n, f) cross sections and calculated results using the EMPIRE-3.1 code.

nucleus formation cross section, $\frac{\sigma_{CN}^{n+^{239}Np}(E_{ex})}{\sigma_{CN}^{n+^{241}Pu}(E_{ex})}$ and $\frac{\sigma_{CN}^{n+^{240}Np}(E_{ex})}{\sigma_{CN}^{n+^{241}Pu}(E_{ex})}$, to obtain the compound nuclear reaction cross section ratios $\frac{\sigma_{f}^{n+^{239}Np}(E_{ex})}{\sigma_{f}^{n+^{241}Pu}(E_{ex})}$ and $\frac{\sigma_{f}^{n+^{240}Np}(E_{ex})}{\sigma_{f}^{n+^{241}Pu}(E_{ex})}$ at similar excitation energies using Eq. (1). The neutron-induced compound nucleus formation cross sections for the present reactions have been determined using the EMPIRE-3.1 code. The $\sigma_{f}^{n+^{241}Pu}(E_{ex})$ cross-section values as a function of excitation energy were used as the reference reaction; these have been derived from Tovesson and Hill [22] by using the neutron separation energy of ^{242}Pu ($S_n = 6.545$ MeV). The ^{239}Np(n, f) and ^{240}Np(n, f) cross sections as a function of excitation energy were obtained over the excitation energy ranges of 16.5–22.5 and 15–22 MeV, respectively, using Eq. (1). The ^{239}Np(n, f) and ^{240}Np(n, f) cross sections as a function of excitation energy are then converted to the equivalent neutron energy ranges of 10.5–16.5 and 9–16 MeV by using neutron separation energies of ^{240}Np ($S_n = 5.066$ MeV) and ^{241}Np ($S_n = 6.13$ MeV), respectively. The present experimental results for the ^{239}Np(n, f) and ^{240}Np(n, f) cross sections as a function of equivalent neutron kinetic energy are shown in Fig. 2 and Fig. 3, respectively.

III. RESULTS AND DISCUSSION

Statistical model calculations have been carried out using the EMPIRE-3.1 [23] code to determine the ^{239}Np(n, f) and ^{240}Np(n, f) cross sections over the equivalent neutron energy range of 1.0–20.0 MeV by considering contributions up to third-chance fission. The EMPIRE-3.1 predictions on neutron-induced fission cross sections are very sensitive to the fission barriers and the level density at the saddle point. In the present work, the fission barrier heights corresponding to all the Np isotopes involved up to third-chance fission in ^{239}Np(n, f) and ^{240}Np(n, f) reactions are obtained from the barrier formula (BF) [24,25]. The fission barrier heights obtained from the BF for various Np isotopes used in EMPIRE-3.1 calculations are listed in Table II. The details of the calculations of fission barrier heights using the BF are presented in the Appendix. The present experimental data have been compared with the recently reported ^{239}Np(n, f) cross sections by Czeszumska *et al.* [2], and adopted cross-section data from JENDL-4.0 [18] (similar to the ENDF/B-VII.1 evaluation) are shown in Fig. 2 along with the calculated cross sections using the EMPIRE-3.1 code. The present experimental results for the ^{239}Np(n, f) cross sections are found to be somewhat higher than the predictions of the EMPIRE-3.1 code, but they reveal expected nuclear structure futures that are similar to those predicted by the EMPIRE-3.1 code. It can be also seen from Fig. 2 that the ^{239}Np(n, f) cross sections of the present work follow closely the recently reported ^{239}Np(n, f) cross sections by Czeszumska *et al.* [2] in the neutron energy range of 13–16 MeV; however, the ^{239}Np(n, f) cross-section values deduced by Czeszumska *et al.* in the neutron energy range of 10–13 MeV are different from the present results. The trend of the JENDL-4.0 data is much lower as compared to the present values of experimental ^{239}Np(n, f) cross sections. However, it is observed that, by reducing the inner and outer barrier heights of the ^{239}Np isotope from the BF predicted values of 5.84 and 5.56 MeV to 5.10 and 5.25 MeV, respectively, the EMPIRE-3.1 code calculations, a better comparison with the present experimental ^{240}Np(n, f) cross sections data is obtained, as shown in Fig. 2 denoted as "best fit." The fission barrier heights corresponding to the best fit to our experimental data are given in Table II, where, the modified fission barrier heights of the ^{239}Np isotope from the BF predictions are shown in rectangular boxes. The ^{240}Np(n, f) cross sections have been measured by employing the HSRM in the equivalent neutron energy range of 9–16 MeV. In this case also the inner and outer barriers for ^{239}Np were modified to the same values of 5.10 and 5.25 MeV for a best fit. The present experimental ^{240}Np(n, f) cross sections are found to compare reasonably well with the EMPIRE-3.1 calculations in

TABLE II. Fission barrier heights for the various Np isotopes used in the EMPIRE-3.1 calculations.

$n + {}^{239}$Np					$n + {}^{240}$Np				
System	Inner barrier height (MeV)		Outer barrier height (MeV)		System	Inner barrier height (MeV)		Outer barrier height (MeV)	
	BF	Best fit	BF	Best fit		BF	Best Fit	BF	Best fit
^{240}Np	6.16	6.16	5.80	5.80	^{241}Np	5.84	5.84	5.60	5.60
^{239}Np	5.84	$\boxed{5.10}$	5.56	$\boxed{5.25}$	^{240}Np	6.16	6.16	5.80	5.80
^{238}Np	6.17	6.17	5.78	5.78	^{239}Np	5.84	$\boxed{5.10}$	5.56	$\boxed{5.25}$
^{237}Np	5.85	5.85	5.50	5.50	^{238}Np	6.17	6.17	5.78	5.78

the neutron energy range of 9–16 MeV, as shown in Fig. 3, for default BF barriers and also for the best fit of ^{239}Np(n, f) barriers.

It may be noted that two different reaction channels such as α and deuteron transfer have been used as surrogate reactions to determine ^{239}Np(n, f) cross sections employing the HSRM in the present work. The angular momentum transfer involved in these two reaction channels are different due to different mass transfer. But it is interesting to note that the present results for the ^{239}Np(n, f) cross section are consistent with EMPIRE-3.1 predictions and also with SRM results in the equivalent neutron energy range of 13–16 MeV [2]. Whether the observed mismatch in ^{239}Np(n, f) cross-section values between experimental results of the SRM and the HSRM for the equivalent neutron energy range of 10–13 MeV is due to an angular momentum effect needs further investigation.

IV. SUMMARY

The neutron-induced fission cross sections of ^{239}Np(n, f) and ^{240}Np(n, f) reactions have been measured in the equivalent neutron energy ranges of 10.5–16.5 and 9–16 MeV, respectively, by employing the hybrid surrogate ratio method. The ^{238}U(^{6}Li, αf)^{240}Np and ^{238}U(^{6}Li, df)^{242}Pu reactions are used as surrogates of n+^{239}Np and n+^{241}Pu neutron-induced reactions for ^{239}Np(n, f) cross-section determinations, while ^{238}U(^{7}Li, αf)^{241}Np and ^{238}U(^{7}Li, tf)^{242}Pu reactions are used as surrogate reactions for n+^{240}Np and n+^{241}Pu reactions for ^{240}Np(n, f) cross-section determinations. The ^{241}Pu(n, f) cross sections as a function of excitation energy have been used as reference reaction in both cases. The present experimental results for the ^{239}Np(n, f) reaction have been compared with the recently reported experimental results by Czeszumska *et al.* [2], EMPIRE-3.1 code calculations, and the evaluated cross-section data obtained from the JENDL-4.0 nuclear data library. The agreement between the two experimental measurements is rather satisfactory and consistent with the EMPIRE-3.1 calculations for the neutron energy range of 13–16 MeV. Below 13 MeV, the present results follow the EMPIRE-3.1 calculations; however, the Czeszumska *et al.* data show clear deviation from the present results and the EMPIRE-3.1 calculations. The evaluated ^{239}Np(n, f) cross-section values by the JENDL-4.0 library are much lower as compared to the present experimental results as well as the results of Ref. [2]. The observed discrepancy between the two experimental measurements suggests the need for more experimental measurements in the neutron energy range from 5 to 13 MeV to understand the ^{239}Np(n, f) cross sections as a function of neutron energy. The ^{240}Np(n, f) cross sections have been measured in the neutron energy range of 9–16 MeV. The present experimental results on ^{240}Np(n, f) cross sections are found to be consistent with the EMPIRE-3.1 calculations.

ACKNOWLEDGMENTS

The authors thank the operating staff of the BARC-TIFR Pelletron Accelerator Facility, for smooth operation of the accelerator during the experiment. We are also thankful to Drs. D. C. Biswas, Bency John, S. Santra, Y. K. Gupta, and L. S. Danu for their interest in this work and the help they provided during the experiment.

APPENDIX

Calculation of fission cross sections are very sensitive to fission barriers and the level density at the saddle point. Due to shell corrections, the fission barriers gets split into two barriers: an inner barrier V_a and an outer barrier V_b for actinide nuclei. It is shown in the work of Gupta and Satpathy [26], which is based on the celebrated Hugenholtz–Van Hove theorem [27], that the fission barrier $V_{i=a/b}$ of a nucleus (A, Z, N) is given by an analytical formula [24]

$$V_i = a_s B_{si} A^{2/3} + a_c B_{ci} \frac{Z^2}{A^{1/3}} + \pi Z + \nu N + k + 0.5[1 + (-1)^Z]\delta_z + 0.5[1 + (-1)^N]\delta_n.$$

The first two terms are surface and Coulomb terms with inclusion of deformation along the fission path. The value of the parameters are given by $a_s = 19(1 - 2.84[\frac{N-Z}{A}]^2)$ MeV and $a_c = 0.72$ MeV. The changes of surface and Coulomb terms B_{si} and B_{ci} are taken from the work of Brack *et al.* [28] and their values are listed in Table III. The next three terms are the microscopic ones and satisfy the Hugenholtz–Van Hove theorem. The last two terms denote pairing effects. The five associated parameters π, ν, k, δ_z, and δ_n are obtained by least-squares fitting to the fission barrier data given by Bjornholm and Lynn for $Z = 89$ to $Z = 98$ are also given in Table III. By using the above expression, the fission barriers for various systems have been calculated in the present work.

TABLE III. List of parameters for the barrier formula.

$i = a/b$	a	b
B_{si}	0.0317	0.1029
B_{ci}	−0.0165	−0.0626
π (MeV)	0.1199	0.2497
ν (MeV)	0.0132	0.0650
k (MeV)	−0.1553	−0.2088
δ_z(MeV)	−0.3224	−0.2183
δ_n (MeV)	−10.2761	−28.8118

[1] J. E. Escher, J. T. Burke, F. S. Dietrich, N. D. Scielzo, I. J. Thompson, and W. Younes, Rev. Mod. Phys. **84**, 353 (2012).
[2] A. Czeszumska *et al.*, Phys. Rev. C **87**, 034613 (2013).
[3] J. D. Cramer and H. C. Britt, Phys. Rev. C **2**, 2350 (1970).
[4] H. C. Britt and J. D. Cramer, Phys. Rev. C **2**, 1758 (1970).
[5] J. J. Ressler *et al.*, Phys. Rev. C **83**, 054610 (2011).
[6] C. Plettner *et al.*, Phys. Rev. C **71**, 051602(R) (2005).
[7] J. T. Burke *et al.*, Phys. Rev. C **73**, 054604 (2006).
[8] V. V. Desai *et al.*, Phys. Rev. C **87**, 034604 (2013).

[9] B. K. Nayak, A. Saxena, D. C. Biswas, E. T. Mirgule, B. V. John, S. Santra, R. P. Vind, R. K. Choudhury, and S. Ganesan, Phys. Rev. C **78**, 061602(R) (2008).
[10] B. F. Lyles, L. A. Bernstein, J. T. Burke, F. S. Dietrich, J. Escher, and I. Thompson, Phys. Rev. C **76**, 014606 (2007).
[11] V. F. Weisskopf and D. H. Ewing, Phys. Rev. **57**, 472 (1940).
[12] S. R. Lesher *et al*., Phys. Rev. C **79**, 044609 (2009).
[13] M. Petit *et al*., Nucl. Phys. A **735**, 345 (2004).
[14] G. Kessedjian *et al*., Phys. Lett. B **692**, 297 (2010).
[15] J. E. Escher and F. S. Dietrich, Phys. Rev. C **74**, 054601 (2006).
[16] S. Chiba and O. Iwamoto, Phys. Rev. C **81**, 0446042010.
[17] M. B. Chadwick *et al*., Nucl. Data Sheets **107**, 2931 (2006).
[18] K. Shibata *et al*., J. Nucl. Sci. Technol. **48**, 1 (2011).
[19] Z. Ge, Z. Zhao, H. Xia, Y. Zhuang, T. Liu, J. Zhang, and H. Wu, J. Korean Phys. Soc. **59**, 1052 (2011).
[20] Y. K. Gupta *et al*., Phys. Rev. C **84**, 031603(R) (2011).
[21] V. V. Parkar, K. Mahata, S. Santra, S. Kailas, A. Shrivastava, K. Ramachandran, A. Chatterjee, V. Jha, and P. Singh., Nucl. Phys. A **792**, 187 (2007).
[22] F. Tovesson and T. S. Hill, Nucl. Sci. Eng. **165**, 224 (2010).
[23] M. Herman *et al*., Nucl. Data Sheets **108**, 2655 (2007).
[24] S. K. Gupta and A. Saxena, in Proceedings of 8th Korean Nuclear Data Workshop, Pohang, 25–26 August 2005.
[25] S. Bjornholm and J. E. Lynn, Rev. Mod. Phys. **52**, 725 (1980).
[26] S. K. Gupta and L. Satpathy, Z. Phys. A **326**, 221 (1987).
[27] N. H. Hugenholtz and W. Van Hove, Physica (Utrecht) **24**, 363 (1958).
[28] M. Brack *et al*., Rev. Mod. Phys. **44**, 320 (1972).